Arabian Journal of Chemistry (2021) **14**, 103227

King Saud University

Arabian Journal of Chemistry

www.ksu.edu.sa
www.sciencedirect.com

ORIGINAL ARTICLE

Cellulosic biomass biocomposites with polyaniline, polypyrrole and sodium alginate: Insecticide adsorption-desorption, equilibrium and kinetics studies

Qurat-ul-ain Khalid [a], Amina Khan [a], Haq Nawaz Bhatti [a,*], Sana Sadaf [b], Abida Kausar [c], Siham A. Alissa [d], Mona K. Alghaith [d], Munawar Iqbal [e,*]

[a] *Department of Chemistry, University of Agriculture, Faisalabad, Pakistan*
[b] *Punjab Bioenergy Institute, University of Agriculture, Faisalabad, Pakistan*
[c] *Department of Chemistry, Government College Women University Faisalabad, Pakistan*
[d] *Chemistry Department, College of Science, Princess Nourah bint Abdulrahman University, Riyadh, Saudi Arabia*
[e] *Department of Chemistry, The University of Lahore, Faisalabad, Pakistan*

Received 30 December 2020; accepted 16 May 2021
Available online 21 May 2021

KEYWORDS

Insecticide;
Cellulosic biomass;
Biocomposites;
Adsorption-desorption;
Kinetics

Abstract This work was designed to synthesize and characterize biocomposites for the adsorptive elimination of insecticide (nitenpyram). Different biocomposites were synthesized of polyaniline (PAN-PH), polypyrrole (PPY-PH) and sodium alginate (Na-Al-PH) with cellulosic biomass of peanut husk (PH), which was characterized fourier-transform infrared spectroscopy (FTIR), pH_{pzc} and scanning electron microscope (SEM). In batch mode, different variables, i.e., contact time, pH, temperature, NP (nitenpyram) concentration and adsorbent dose effects were investigated. The adsorption capacities of PH, PAN-PH, PPY-PH and Na-Al-PH were recorded to be 13.0, 14.43, 13.61 and 11.91 (mg/g), respectively at 30 °C, 60 min contact time, 0.05 g and 2.0 pH. Pseudo second order kinetic and Freundlich isotherm models best explained the NP adsorption data. An exothermic adsorption nature of NP adsorption was observed on to PH, PAN-PH, PPY-PH and Na-Al-PH. The NP desorption was efficient with NaOH and biocomposites are competent for the adsorptive removal of NP, which can utilized for NP remediation in effluents.

* Corresponding authors.
E-mail addresses: hnbhatti2005@yahoo.com (H.N. Bhatti), bosalvee@yahoo.com (M. Iqbal).
Peer review under responsibility of King Saud University.

Production and hosting by Elsevier

1. Introduction

Environmental pollution is becoming a serious threat to the society and it must be genuinely analyzed. Water pollution is of major concern among the different kinds of environmental pollutions due to its extensive utilization and ability to solubilize a wide variety of chemicals including intense toxicants released by different industries. Advanced

https://doi.org/10.1016/j.arabjc.2021.103227
1878-5352

countries have made environmental strategies that zero synthetic compounds ought to be discharged into marine environment. The quality of water in natural reservoirs is falling down with every passing day due to continuous introduction of unwanted synthetics chemicals in them. The primary sources of water pollution are agricultural and industrial wastes (Bokhari et al., 2020; Jamil et al., 2020a; Jamil et al., 2020b; Jamil et al., 2020c; Shoukat et al., 2017; Sohail et al., 2020).

Application of pesticides and insecticide on crops is a common practice of farmers in agriculture sector in order to protect the cultivated crops from the attack of harmful insects. Narrow spectrum pesticides are those that target only particular pest, but many pesticides are broad spectrum and their impact can be seen infinite to the large extent (Ramli et al., 2019). Nitenpyram is very common and abundantly utilized neonicotinoid pesticide and it is considered lethal to non-target aqueous microorganisms. Neonicotinoid is a synthetic structure of nicotine that is used to secure yields against penetrating sucking pests. These pesticides are directly connected to the soil and are transported into ground water. The extensive utilization of these pesticides for high yielding harvests has shockingly created numerous ecological issues and environmental upsets (Bhatti et al., 2020; Yuan et al., 2019). The wide utilization of pesticides and their introduction into water poses negative impacts for biological systems because these pesticides are considered as persistent organic pollutants (POPs). The pollution of water sheds by these pesticides is an alarming issue for the researchers over a time of years (Abbas et al., 2021; Adetutu et al., 2020; Igbanoi et al., 2019; Iqbal et al., 2019; Ukpaka et al., 2020).

The techniques utilized for the purification of water include ozonation, catalytic and photocatalytic degradation, liquid extraction, strong phase extraction, nano-filtration film and adsorption, while for specifically NP removal include electro-catalytic degradation, electrochemical oxidation and photodegradation (Benabdallah et al., 2017; Daij et al., 2017; Djehaf et al., 2017; Iqbal and Khera, 2015; Jamal et al., 2015; Qureshi et al., 2015; Sasmaz et al., 2018; Sasmaz et al., 2019; Sayed, 2015; Sinanoglu and Sasmaz, 2019). To date, different techniques (biological, chemical and physical) have been applied for the elimination of nitenpyram, i.e., *Actinomycetes Rhodococcus* was utilized for the remediation of NP via a hydroxylation pathway in surface water and calcium alginate immobilized cells removed 87.11% nitenpyram in 8 days (Dai et al., 2021). Similarly, g-C_3N_4/WO_3/AgI was prepared and used for the removal of nitenpyram. The NP removal was excellent using prepared catalyst, which was spoused to solar light (Tang et al., 2020). On the same line, a photocatalytic degradation of nitenpyram was performed using Ag_3PO_4 (sulfate-doped) under visible light exposure and the Ag_3PO_4 (-sulfate-doped) furnished promising efficiency for the removal of nitenpyram along with other pesticides and insecticides (Lee et al., 2020). The adsorptive removal has also been reported for nitenpyram using modified resin with proline and 48–86% nitenpyram removal was achieved under variables conditions (Wu et al., 2014). Among different approaches, the adsorptive removal offers various advantages versus others, i.e., selective, effective (even at very minute level of contaminant), regeneration ability of the adsorbents and cost effective (Abbas et al., 2021; Awwad et al., 2021a; Awwad et al., 2021b; Elsherif et al., 2021; Ismail et al., 2021; Ukpaka and Eno, 2020; Ukpaka et al., 2020). Different type of adsorbents like eucalyptus, citrus, barley, mustard, sugarcane bagasse, rice husk, saw dust and peanut husk are applied for the adsorption of contaminants. Among all these, peanut husk showed good adsorption potential. However, it has been observed that these adsorbents have very low adsorptive removal efficiency in natural/raw form. Modification of adsorbents with biological moieties displayed auspicious competence for the elimination of different pollutants (Demarchi et al., 2019; Kovačević et al., 2019; Marinescu et al., 2019).

In view of competitive elimination efficiency of composites, the biocomposites based on cellulosic biomass with polyaniline, polypyrrole and sodium alginate were fabricated and utilized as an adsorbent for NP insecticide removal. Process variables were studied for optimal adsorption of NP and desorption was also studied to regenerate the adsorbent.

2. Material and methods

2.1. Chemical and reagents

The chemicals and reagents, i.e., HCl (37%), aniline (≥99.7%), methanol (≥95%), pyrrole (99%), acetic acid (≥98.99%), ammonium persulfate (≥98%), sulfuric acid (98%), KNO_3 (≥98.0%), NaCl (≥98.5%), $CaCl_2$ (≥98.0%) and $AlCl_3$ (98%) were acquired from Sigma-Aldrich.

2.2. Preparation of biomasses

Different types of agrowaste i.e., mustard biomass, saw dust, peanut husk, eucalyptus biomass, citrus biomass, sugarcane bagasse, barley husk and rice husk were obtained from local forms, FSD, Pakistan. Collected agrowastes were chopped and then, washed with double distilled water, dried in open atmosphere and in oven at 60 °C. The dried agrowastes were crushed and sieved to ≤ 300 μm size (oct-digital 4527–01). The prepared agrowastes were screened for adsorptive removal of NP to select one with maximum adsorption potential. Stock solution (500 ppm) of NP was prepared in distilled water and various dilutions (5–25 ppm) were made by utilizing this stock solution.

2.3. Synthesis of biocomposites

For the preparation of polyaniline and peanut husk biocomposite (PAN-PH), 5 mL aniline in 250 mL of 1 M hydrochloric acid was dissolved and placed the beaker in an ice bath to cool the mixture and ammonium persulfate was dropped over a period of 30–40 min with continuous stirring. After adding ammonium persulfate solution, agitated for 120 min and kept next 12 h at room temperature. Next day, filtered the suspension and rinsed it with distilled water and methanol for the removal of the monomer of polyaniline (Gupta et al., 2004). Polyaniline of dark green color was observed. Next step was to prepare the EB form of polyaniline. Took 5 g of polyaniline and dissolved in 100 mL of 0.5 M sodium hydroxide (NaOH), then stirred the mixture for 3 h and filtered. Dried it in oven at 60 °C, took 50 mL of formic acid and added 0.5 g EB form of polyaniline and mixed it well for 10–15 min. Then, added 5 g of pH in the above mixture and stirred it for 2.5 h. Left it overnight and dried it in open atmosphere.

For the preparation of polypyrrole and penut husk biocomposite (PPY-PH), 100 mL of pyrrole and 3 g of pH was mixed and left it overnight. On next day, 0.5 M $FeCl_3$ was supplemented and left the system overnight. Next day, filtered and rinsed it with distilled water and methanol. After filtration, composite was dried in oven at 60 °C (Palanisamy et al., 2012).

For the preparation of sodium alginate and peanut husk (Na-Al-PH), 100 mL of distilled water was added in a beaker and heated it for 1 min and 2 g of sodium alginate was supplemented to it by continuous stirring until slurry was formed. A 0.05 M $CaCl_2$ solution was added dropwise in the above mixture and beads of sodium alginate were formed. Beads were saved in $CaCl_2$ solution below 5 ^{0}C (Ishtiaq et al., 2020).

2.4. Batch biosorption studies

The process parameters, i.e., pH (2–9), temperature (303–328 K), adsorbent dose (0.05–0.30), initial pesticide concentration (5–100 ppm) and contact time (5–120 min) on the biosorption of NP was studied (Scheme 1). The batch adsorption study for pesticide was accomplished in 250 mL conical flask by adding adsorbent dose in 50 mL of pesticide solution of specific concentration. By keeping one factor variable and all other constant, different process parameters were optimized. The rate of biosorption was studied by utilizing Eq. (1).

$$q_e = (C_i - C_e)\frac{V}{W} \quad (1)$$

where C_i, q_e, C_e, W and V are representing initial concentration of insecticides, adsorption capacity, equilibrium concentration, mass of adsorbent and volume, respectively.

2.5. Equilibrium modeling

Various models were applied (Langmuir, Temkin, Freundlich, Dubinin Randushkevich, Harkins-Jura) on experimental data for determining mechanism of adsorption process.

2.6. Adsorption kinetics

Data was kinetically analyzed by employing pseudo first order, intra-particle diffusion and pseudo second order kinetics models.

2.7. Thermodynamic study

Different thermodynamics parameters, i.e., ΔG^o, ΔH^o and ΔS^o were calculated evaluate the nature and feasibility of the NP adsorption on to biocomposites.

3. Results and discussion

3.1. Adsorbents efficiency

Screening of different agrowastes for removal of NP was performed by using Mustard (MT), sugar cane bagasse (SB), Citrus (CT), peanut husk (PH), euclyptus (EU), rice husk (RH), saw dust (SD) and barley husk (BA) biomass and outcomes are displayed in Fig. 1. The peanut husk (PH) biomass has maximum adsorption capacity for NP. Therefore, composites of PAN, PPY, and Na-Alg were prepared with PH biomass for further study. Working conditions for screening were adsorbent dose: 0.05 g, pesticide conc.: 25 ppm, temperature: 30 °C, volume of solution: 50 mL, size of adsorbent particle: $\leq$ 300 μm, contact time: 90 min and 120 rpm agitation.

3.2. Process variables impact on NP adsorption

3.2.1. pH impact

pH impact on adsorption of NP using various biocomposites was investigated in 2–9 range. The result indicated that optimum pH for maximum NP adsorption onto native (PH), polyaniline composite (PAN-PH), polypyrrole composite (PPY-PH) and sodium alginate composite (Na-Al-PH) was 2 and the maximum adsorption capacity of PH, PAN-PH, PPY-PH and Na-Al-PH was 12.91, 14.43, 13.61 and 11.91 (mg/g), respectively (Fig. 2). It was observed that acidic pH is viable for maximum adsorption of NP, which is due to the reason that in acidic pH range, the adsorbent surface bears positive charges. The electrostatic attraction in between positively charges adsorbent and pesticide increases and resultantly, the adsorption capacity was enhanced, which could be explained using pH_{pzc} concept. The pH_{pzc} was 7.4 for PH (Fig. 3). At $pH_{pzc} < 7.4$, a positively charged adsorbate molecules attracted towards adsorbent and at $pH_{pzc} > 7.4$, a negatively charged molecules were attracted on the adsorbent surface (Shoukat et al., 2017). Hence, the reduction in removal

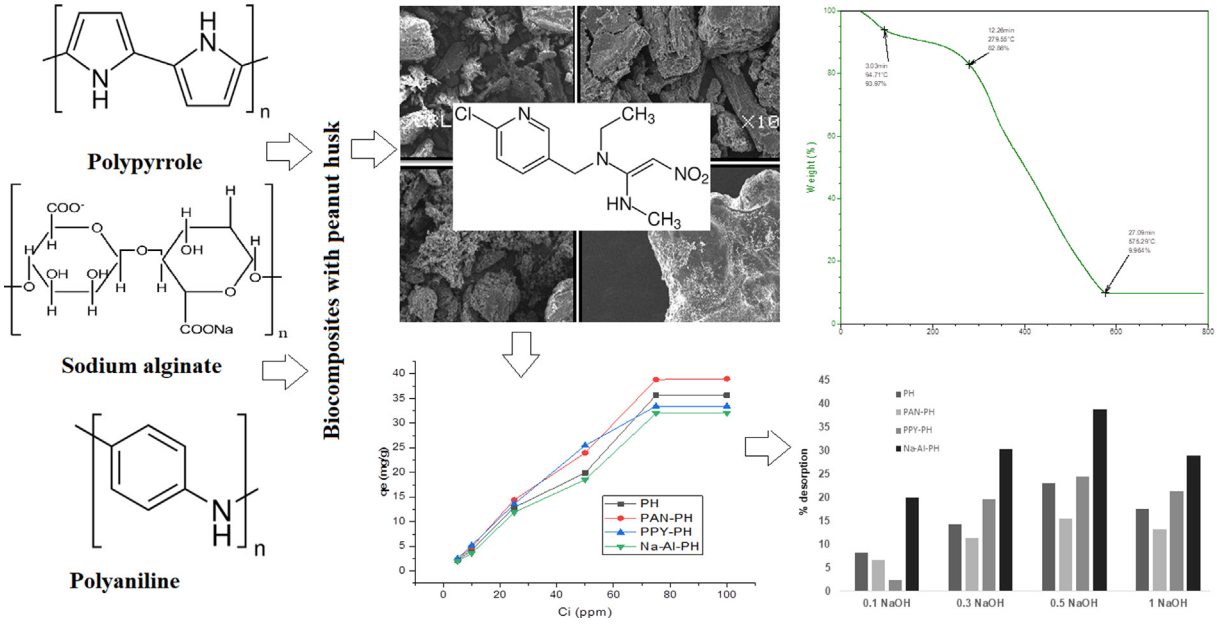

Scheme 1 Schematic presentation of biocomposite preparation and adsorption–desorption studies.

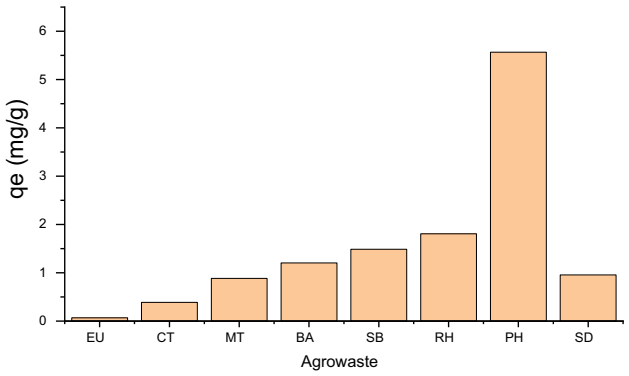

Fig. 1 Screening of different agro wastes for removal of NP from aqueous solution [Adsorbent dose: 0.05 g, insecticide conc: 25 ppm, Temperature: 30 °C, volume: 50 mL, size of biosorbent: ≤ 300 μm, Shaking speed: 120 rpm and contact time: 120 min]

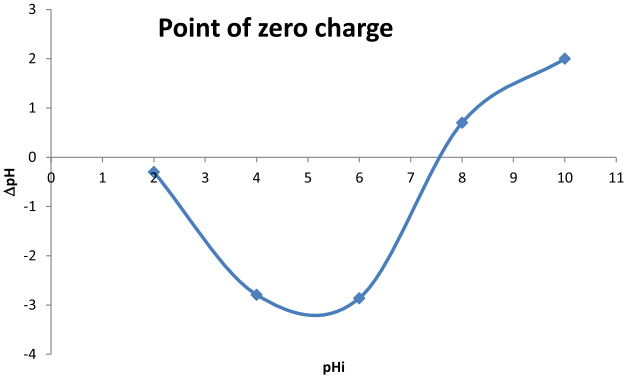

Fig. 2 Point of zero charge determination.

of NP by using all biosorbents was observed with pH change from acidic to basic range.

3.2.2. Adsorbent dose

Amount of adsorbate is a significant factor during elimination process because it finds out the adsorbent potential for a given initial concentration of adsorbate. Experiment was conducted using different biomass dosage and the adsorption showed reverse relation with dose. The optimum adsorbent dose was found to be 0.05 g having maximum adsorption capacity of 12.91, 14.43, 13.62 and 11.91 (mg/g) for PH, PAN-PH, PPY-PH and Na-Al-PH, respectively (Fig. 4). Such a reduction in adsorption capacity with dose may be due to the overlapping of active moieties and resultantly, surface area for the binding of insecticide was diminished. This overlapping of binding sites also leads to the enlarged path length of diffusion which results in decrease in adsorption capacity (Tahir et al., 2017).

3.2.3. Initial concentration

Initial adsorbate concentration is the main driving force during adsorption process and poses significant impact on the removal process, which was studied in 5–100 ppm range and it was observed that adsorption potential of pH and its composites PAN-PH, PPY-PH and Na-Al-PH was increased with the rise in insecticide concentration up to 75 ppm, but from

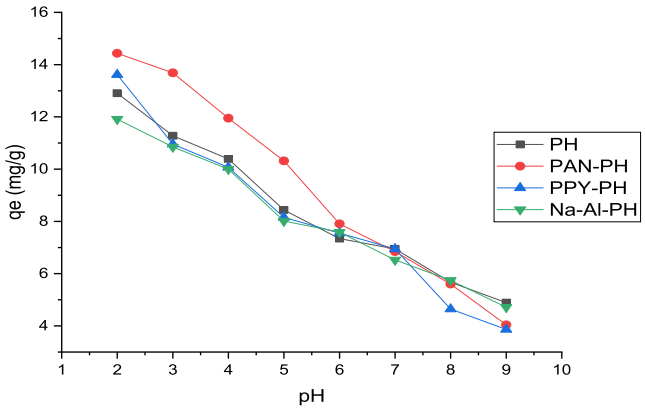

Fig. 3 NP adsorption onto PH, PAN-PH, PPY-PH and Na-Al-PH at different pH [temp: 30 °C, insecticide conc: 25 ppm, adsorbent dose: 0.05 g/50 mL, contact time: 90 min, shaking speed: 120 rpm, size of biosorbent: ≤ 300 μm]

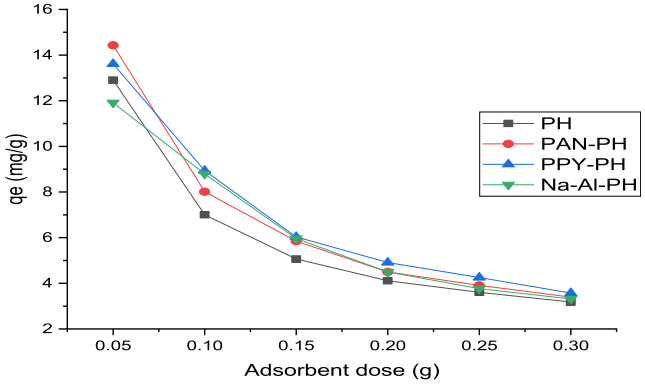

Fig. 4 NP adsorption onto PH, PAN-PH, PPY-PH and Na-Al-PH at different adsorbent dose [temp: 30 °C, insecticide conc: 25 ppm, pH 2, contact time: 90 min, shaking speed: 120 rpm, size of biosorbent: ≤ 300 μm].

75 ppm to 100 ppm, it remains constant (Fig. 5). At initial concentration of 5 ppm, the adsorption capacities of PH, PAN-PH, PPY-PH and Na-Al-P H were 1.99, 2.30, 2.52 and 1.98 (mg/g), respectively and adsorption capacities of these adsorbents increased to 32.05, 39.0, 33.44 and 32.05 (mg/g), respectively at the NP initial concentration of 100 ppm. It is due to the reason that at low initial concentration of insecticide, number of empty binding sites was also higher and percentage removal was high (Tahir et al., 2017).

3.2.4. Temperature

Temperature is also a very significant character in the adsorptive removal of contaminants onto the surface of adsorbents, which was investigated in a 303–328 K range. The PH and its biocomposites adsorptive removal efficiencies were decreased with rise in temperature (Fig. 6). The highest biosorption capacity was achieved at 303 K for the removal of NP. The adsorption capacities of PH, PAN-PH, PPPY-PH and Na-Al-PH was 12.91, 14.43, 13.62 and 11.91 (mg/g), respectively. The decrease in NP adsorption at higher temperature is due to the breakdown of adsorption forces that were

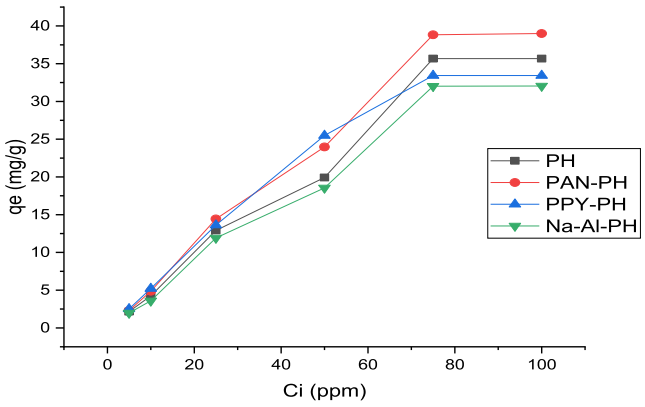

Fig. 5 NP adsorption onto PH, PAN-PH, PPY-PH and Na-Al-PH at different initial concentration of NP [temp: 30 °C, pH 2, adsorbent dose 0.05 g, contact time: 90 min, shaking speed: 120 rpm, particle size ≤ 300 μm].

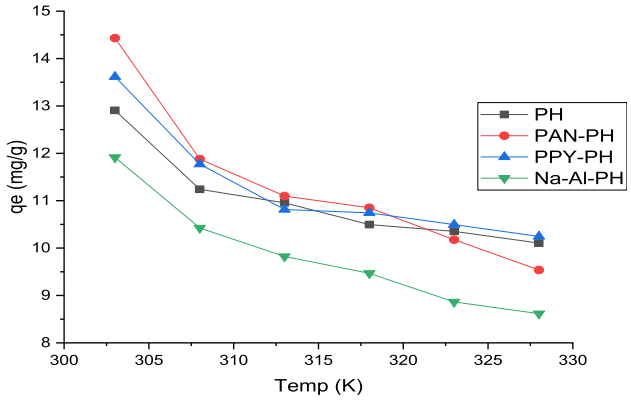

Fig. 6 NP adsorption onto PH, PAN-PH, PPY-PH and Na-Al-PH at different temperature [pH 2, adsorbent dose 0.05 g, contact time: 90 min, initial insecticide conc: 25 ppm, shaking speed: 120 rpm, particle size ≤ 300 μm].

accountable for the binding of NP on the surface (Tahir et al., 2017). At higher temperature bonds are broken down and resultantly, a desorption may occur. The biosorption capacity decreased by changing the surface properties of adsorbent due to demolished active sites at higher temperature (Shoukat et al., 2017).

3.2.5. Contact time

Reaction time between adsorbent and adsorbate required for the uptake of maximum amount of adsorbate onto the surface of adsorbent, which is also a crucial parameter in adsorption process, which was studied in 5–120 min range. It was noted that most of the contaminant molecules get attach onto the adsorbent active sites in short interval of contact time. This shows that adsorption is a fast process. At the initial stage, this removal rate was very fast, then it becomes gradually slow and finally, reached to the constant value, which indicates saturation point. Maximum adsorption was found at contact time 60 min (Fig. 7). The adsorption capacities for PH, PAN-PH, PPY-PH and Na-Al-PH at optimum contact time was 15.74, 15.74, 15.03 and 12.52 (mg/g), respectively. The process of

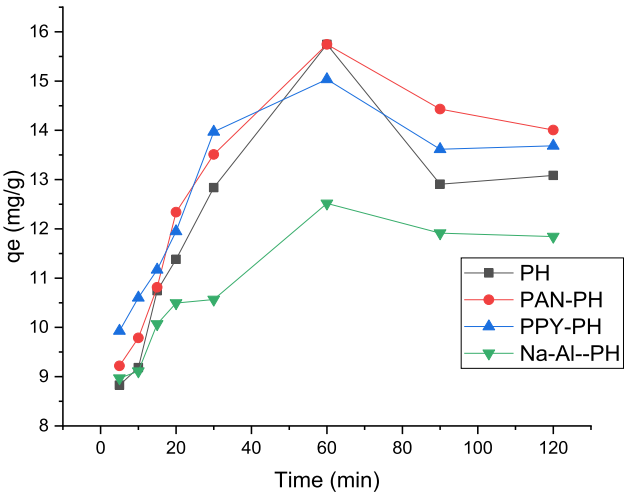

Fig. 7 NP adsorption onto PH, PAN-PH, PPY-PH and Na-Al-PH at different time intervals [temp: 30 °C, insecticide conc: 25 ppm, pH 2, adsorbent dose 0.05 g, shaking speed: 120 rpm, size of biosorbent: ≤ 300 μm].

adsorption was high initially due to the presence of more free binding sites, which became saturated after sometime by attachment of NP. After that, these already occupied binding sites repel the upcoming contaminant ions and the process of adsorption becomes slow and the different in concentration between solid and liquid phases was also changed with the passage of time (Shoukat et al., 2017).

3.3. Kinetic modeling

The kinetics of NP onto biocomposites was studied employing pseudo first order, intra particle diffusion and pseudo second order kinetic models (Ho and McKay, 1999; Lagergren, 1898; Weber and Morris, 1963).

Pseudo first order showed the relationship among the NP removal with time. Pseudo first order model showed that change in NP concentration with time is analogous to power one. The relation of pseudo first order is depicted in Eq. (2).

$$\log(q_e - q_t) = \log q_e - \frac{k_i t}{2.303} \tag{2}$$

where q_e is the adsorption capacity, q_t is the amount of insecticide adsorbed at the time t, K_1 is the adsorption constant (L min^{-1}). The R^2 values obtained after application of pseudo first order kinetic model were 0.363, 0.61, 0.498 and 0.909 for PH, PAN-PH, PPY, PH and Na-Al-PH, respectively and such low values of R^2 show that this model is not best fit onto experimental data (Table 1), which also confirms the poor fitness of model. The q_e calculated from model is also not in agreement with q_e determined experimentally. Pseudo second order kinetics shows the adsorption phenomena with complete extent of contact time, with chemiosorption being rate limiting step. The relation is depicted in Eq. (3).

$$\frac{t}{q_t} = \frac{1}{k_2} q_e^2 + \frac{1}{q_e}(t) \tag{3}$$

where t is the contact time, k_2 is rate constant for pseudo second order, q_e is equilibrium amount of insecticide, q_t is insec-

Table 1 Kinetics parameters for the adsorptive removal of Nitenpyram (NP) on to PH, PAN-PH, PPY-PH and Na-Al-PH biocomposites.

	PH	PAN-PH	PPY-PH	Na-Al-PH
First order				
K_1 (L/min)	0.00898	0.0131	0.0113	0.01612
q_{cal} (mg/g)	5.16	4.91	3.61	3.21
q_{exp} (mg/g)	15.744	15.744	15.035	12.517
R^2	0.363	0.61	0.498	0.909
Second order				
K_2 (g/mg min)	0.0294	0.0203	0.0328	0.0290
q_{cal} (mg/g)	13.64	14.81	14.14	12.67
q_{exp} (mg/g)	15.744	15.74	15.035	12.516
R^2	0.989	0.994	0.996	0.998
Intraparticle diffusion				
K_{pi} (mg/g $min^{1/2}$)	0.552	0.626	0.466	0.374
C_i	8.57	8.77	9.734	8.47
R^2	0.576	0.701	0.637	0.799

ticide amount eliminated at time t. Data shows that the R^2 for second order kinetic model was 0.989, 0.994,0.996 and 0.998 in case of high PH, PAN-PH, PPY-PH and Na-Al-PH, respectively (Table 1). The calculated adsorption capacity is compatible with expérimental adsorption capacity. Hence, the pseudo second order kinetic model best explained the NP adsorption on to biocomposites.

3.3.1. Intraparticle diffusion model

Various stages are taking part in the movement of insecticide towards the adsorbent surface from the medium in the adsorption phenomena. To study the diffusion mechanism of biosorption process, it is very essential to study intraparticle diffusion model. Bulk diffusion indicates the first stage, in which molecules extend the surface of the adsorbent. In the next stage, molecules spread on the exterior surface of the adsorbent and it is considered as film diffusion. In third stage, molecules move towards the inner side and this considered as intra particle diffusion. In final stage, chemical reaction occurs and adsorbate get adsorbed on the adsorbent active sites (Eq. (4)).

$$q_{t=}k_{pi}t_{1/2} + C_i \tag{4}$$

where C_i is the intercept, K_{pi} is the constant. In this case, the value of R^2 are very low (the value of R^2 for PH, PAN-PH, PPY-PH and Na-Al-PH are 0.576, 0.701, 0.637 and 0.799, respectively) (Table 1) which show poor fittness of this model onto experimental data.

3.4. Isotherm modeling

The biosorption isotherm gives important information to understand the surface behavior of biosorbent. Different models are used to evaluate the biosorption process, i.e., Langmuir, Temkin, Freundlich, Dubinin-Radushkevich, and Harkins-Jura models (Dubinin and Raduskhevich, 1947; Freundlich, 1906; Harkins and Jura, 1944; Langmuir, 1918; Temkin, 1940). The Langumir biosorption isotherm suggested that biosorption occur on homogenous biosorption surface. Further it shows that biosorption leads to the monolayer of biosorbate molecules on biosorbent surface (Eq. (5)).

$$\frac{C_e}{q_e} = \frac{1}{q_{max}}.b + \frac{C_e}{q_{max}} \tag{5}$$

where q_m is maximum biosorption capacity, b is Langmuir constant, C_e is concentration of insecticide at equilibrium and q_e is biosorption capacity at equilibrium. The Langmuir model does not exhibit the applicability for biosorption of NP on peanut husk (PH) and its biocomposites (PAN-PH, PPY-PH, Na-Al-PH) because the value of R^2 is not acceptable (Table 2). Freundlich isotherm is viable for multilayer adsorption and it exhibits the heterogeneous behavior of adsorbent surface and shows the attraction among biosorbed molecules and variable distribution of biosorption heat on adsorbent surface (Eq. (6)).

$$log\ \ q = \log K_F + \frac{1}{n} logCe \tag{6}$$

where q_e and C_e is the biosorption capacity and insecticide concentration at equilibrium, K_F is Freundlich biosorption constant and n shows the adsorption linearity. If $n = 1$ biosorption is linear, $n < 1$ showed chemiosorption phenomena and $n > 1$ showed is a physical process (Shoukat et al., 2017). Increase in value of K_F showed that percentage removal increases with rise in temperature. The value of K_F and R^2 are 0.904 and 0.964 for PH, whereas these values for K_F and R^2 were 1.094 and 0.957 for PAN-PH and 1.448 and 0.956 for PPY-PH and 0.735 and 0.963 for Na-Al-PH, respectively, which shows best applicability of this model. The value of n is greater > 1, biosorption is favorable. Hence, the Freundlich model is fitted best on the adsorption of NP by peanut husk and its biocomposites PH, PAN-PH, PPY-PH and Na-Al-PH (Table 2).

The Temkin model indicates an equivalent diffusion of binding energies on the interchanging sites on the surface. The diffusion of these energies based on the number of active moieties (binding sites) on the insecticide molecule and the adsorbent layer (Eq. (7)).

$$q_e = BlnA + BlnC_e \tag{7}$$

where A is binding constant at equilibrium, B is heat of biosorption. The value of R^2 for PH, PAN-PH, PPY-PH and Na-Al-PH are 0.903, 0.938, 0.967 and 0.913, respectively,

Table 2 Isotherm modeling parameters for the adsorptive removal of Nitenpyram (NP) on to PH, PAN-PH, PPY-PH and Na-Al-PH biocomposites.

Isotherms	PH	PAN-PH	PPY-PH	Na-Al-PH
Langmuir				
$q_{m\ cal}$ (mg/g)	131.579	129.87	62.893	138.889
$q_{m\ exp}$ (mg/g)	35.67185	38.00192	33.43762	32.05098
B	0.00667	0.00847	0.01984	0.00516
R_L	0.599	0.541	0.335	0.659
R^2	0.351	0.386	0.839	0.254
Freundlich				
K_F	0.904	1.094	1.448	0.733
n	1.064	1.059	1.213	1.49
R^2	0.964	0.957	0.956	0.963
Temkin				
A	0.309	0.342	0.41	0.284
B	11.66	12.99	10.64	10.62
R^2	0.903	0.938	0.967	0.913
Harkins-Jura				
A	7.519	8.849	11.111	6.098
B	1.546	1.506	1.537	1.577
R^2	0.677	0.628	0.639	0.715
D-R				
q_m (mg/g)	21.68	25.34	23.32	19.12
β (mol^2kJ^{-2})	0.000004	0.000004	0.000003	0.000005
E ($kJmol^{-1}$)	0.3536	0.3536	0.4082	0.4472
R^2	0.771	0.817	0.824	0.737

which revealed the Temkin model also fitted well on the adsorption of NP by PH and its biocomposites (PAN-PH, PPY-PH and Na-Al-PH). The values of R^2, A and B are presented in Table 2. Harkins-Jura model was employed to describe the multilayer biosorption because of heterogeneous diffusion (Eq. (8)).

$$\frac{1}{qe^2} = \left(\frac{B}{A}\right) - \left(\frac{1}{A}\right) log C_e \tag{8}$$

The R^2 values for PH, PAN-PH, PPY-PH and Na-Al-PH were 0.677, 0.628, 0.639 and 0.715, which is not in acceptable range, hence, Harkins-Jura did not fit to the experimentation data (Table 2). The model indicated that PH biowaste does not contain heterogeneous pore diffusion. D-R model shows non-uniform biosorption capacity of biomass. The free energy and biosorption properties can be found by using D-R model (Eq. (9)).

$$\ln q_e = \ln q_m - \beta\varepsilon^2 \tag{9}$$

where q_m is theoretical saturation potential, ε is Polanyi potential (Eq. (10)), T and R are the temperature (absolute) and gas constant.

$$\varepsilon = RTln\left(1 + \frac{1}{C_e}\right) \tag{10}$$

E (Eq. (11)) is free energy of adsorption. The regression coefficient values of PH, PPY-PH, Na-Al-PH and PAN-PH are 0.771, 0.817, 0.824 and 0.737, respectively. These values revealed that this model did not fit best on the biosorption of NP by PH and its composites (Table 2).

$$E = \frac{1}{(2\beta)^{1/2}} \tag{11}$$

3.5. Thermodynamics study

To understand the behavior of adsorption, the thermodynamics parameters, i.e., ΔG ΔH and ΔS were computed (Eq. (12)). k_d is a coefficient and Eq. (13) is used to calculate the K_D. Where, q_e and C_e are adsorption capacity and equilibrium concentration, respectively and final form is presented in Eq. (14).

$$\Delta G^0 = -RTlnk_d \tag{12}$$

$$K_d = \frac{q_e}{C_e} \tag{13}$$

$$lnK_d = \frac{\Delta S}{R} - \frac{\Delta H}{RT} \tag{14}$$

Slop and intercept can be calculated from ΔH and ΔS. The ΔG positive indicates a non-spontaneous process and so on. This indicates that by increasing the temperature, the spontaneity of the reaction reduced. The enthalpy positive value showed that sorption phenomena is endothermic, while negative value of enthalpy showed that sorption phenomena is exothermic. From the Table 3, the adsorption capacity was decreased with temperature. The adsorption of NP on PH, PAN-PH, PPY-PH and Na-Al-PH are exothermic reaction because of negative value of ΔH. The negative value of entropy showed the decrease in randomness during adsorption of NP on PH and its biocomposites.

3.6. Desorption study

Desorption is very significant to recover the adsorbent and adsorbate and for reusability of adsorbent. Desorption study was performed by using the NP loaded PH biomass and its

Table 3 Thermodynamics parameters for the adsorptive removal of Nitenpyram (NP) on to PH, PAN-PH, PPY-PH and Na-Al-PH biocomposites.

Adsorbents	Tem (K)	ΔG	ΔH	ΔS
PH		kJ/mol	kJ/mol	$Jmol^{-1}$ K^{-1}
	303	−0.164	−13.21	−43.91
	308	0.518		
	313	0.646		
	318	0.855		
	323	0.931		
	333	1.057		
PAN-PH	303	−0.785	–23.02	−7.46
	308	0.255		
	313	0.586		
	318	0.702		
	323	1.009		
	333	1.317		
PPY-PH	303	−0.045	−15.98	−5.23
	308	0.029		
	313	0.071		
	318	0.075		
	323	0.087		
	333	0.099		
Na-Al-PH	303	0.236	−17.06	−57.73
	308	0.858		
	313	1.132		
	318	1.309		
	323	1.608		
	333	1.752		

composites. In this experiment, various concentration (0.1 N, 0.3 N, 0.5 N, 1 N) of NaOH and HCl was used to desorb the adsorbed NP to regenerate the adsorbent. The results shown in Fig. 8 revealed that desorption of NP from PH, PAN-PH, PPY-PH and Na-Al-PH was increased with NaOH concentration (up to 0.5 N) and later, it was decreased. The effective desorption (%) was due to more number of negative charges on the surface of sorbent, that generate repulsive surface among the adsorbent and adsorbed insecticide.

3.7. Characteristics of the adsorbents

SEM analysis is employed to overview the morphological characteristics of biocomposites such as particle shape and porosity (Awwad et al., 2020a) since adsorbent is dependent to surface characteristics of the adsorbents. Higher the number of pores, higher will be the adsorption efficiency of adsorbents. SEM images of PH, PPY-PH, PAN-PH and Na-Al-PH are displayed in Fig. 9. Results specified that PAN-PH is more porous among all of the adsorbents and Na-Al-PH is least. Hence, the order of adsorption capacity of all the adsorbent was as follows, PAN-PH > PPY-PH > PH > Na-Al-PH. FT-IR spectra of all the adsorbents is presented in Fig. 10. FT-IR analysis identify the active moieties response for the binding of adsorbate (Amer and Awwad, 2021; Awwad et al., 2021b; Awwad et al., 2020b). FT-IR spectrum of pH showed a broad peak at 3334 cm^{-1} that is due to the OH stretching and a peak at 2920 cm^{-1} revealed the presence of

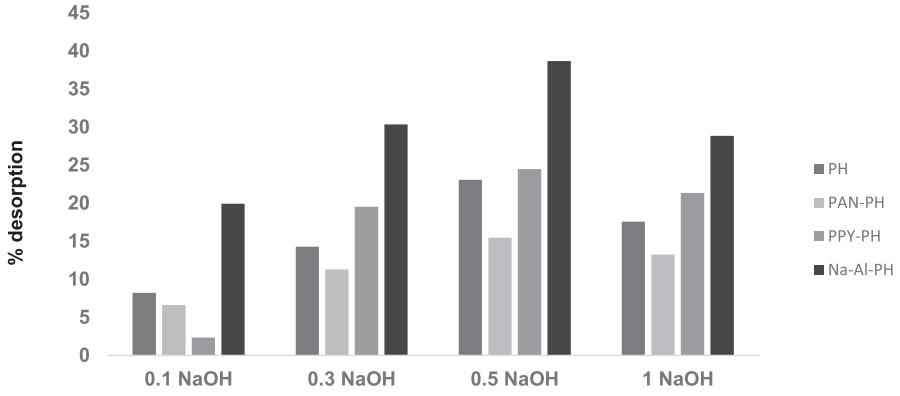

Fig. 8 Desorption of NP from PH, PAN-PH, PPY-PH and Na-Al-PH biocomposite [temp: 30 °C, adsorbent dose 0.05 g, shaking speed: 120 rpm).

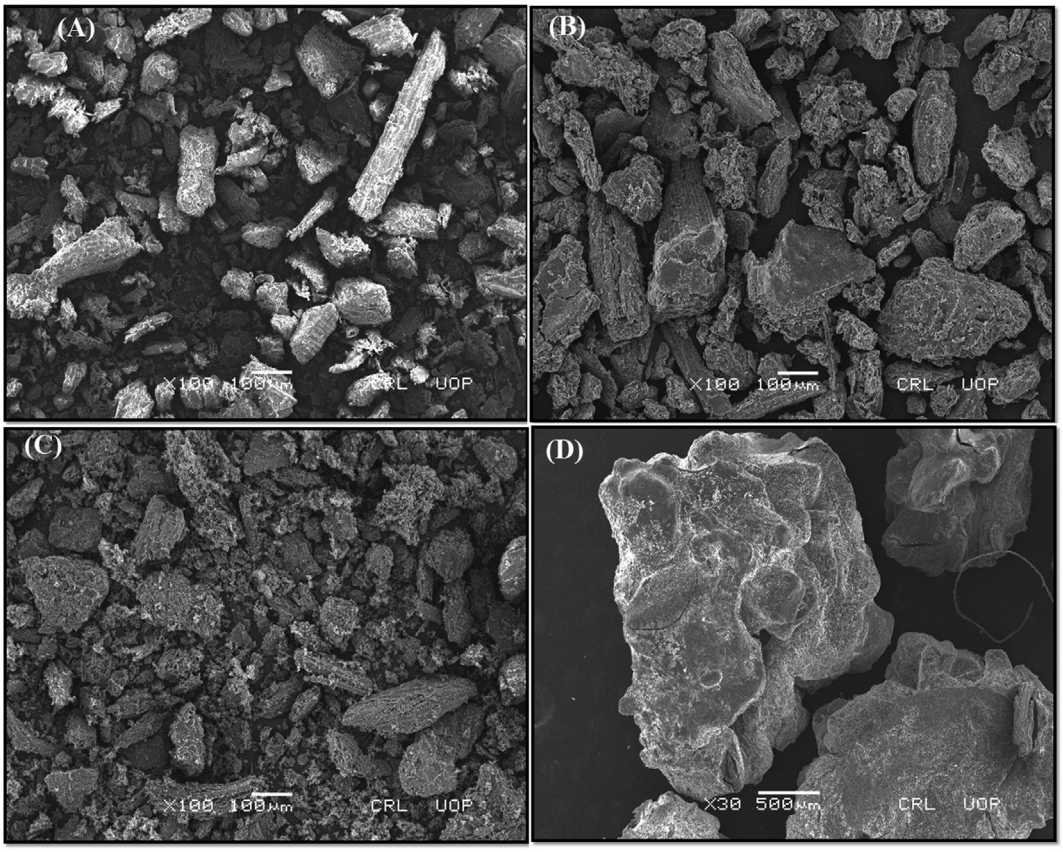

Fig. 9 SEM analysis of (A) PH (B) PAN-PH (C) PPY-PH (D) Na-Al-PH biocomposite.

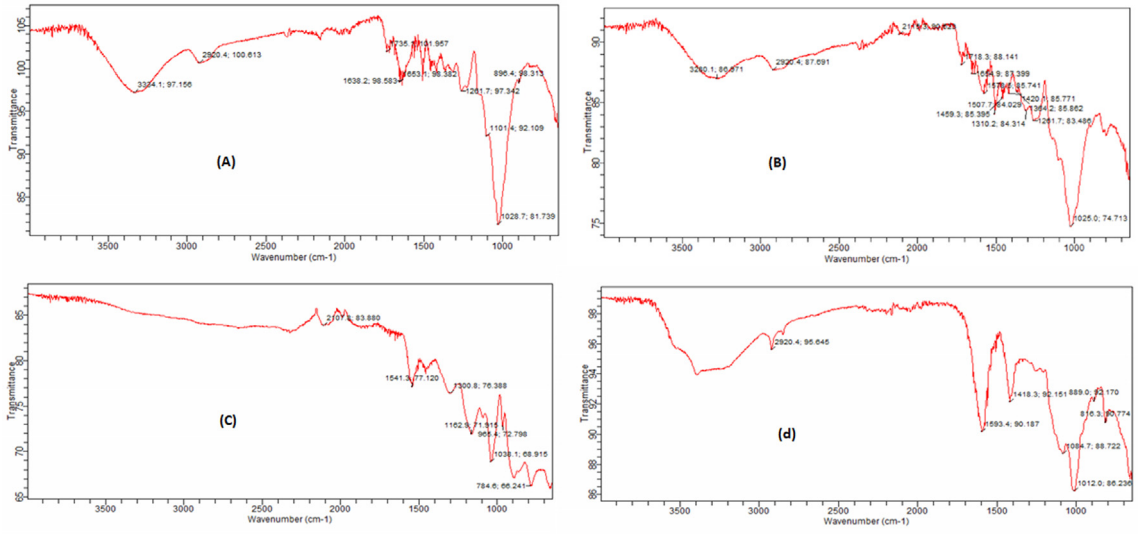

Fig. 10 FT-IR spectra of (A) PH (B) PAN-PH (C) PPY-PH (D) Na-Al-PH biocomposite.

CH group in the structure of PH. A sharp peak at 1028 cm^{-1} is due to the R-O stretching vibration. A peak at 1638 cm^{-1} indicates the C = O group. In the spectrum of PPY-PH a band appeared at 1541 cm^{-1} is an indicative of amide group. FT-IR spectra of Na-Alginate-PH showed bands at 3233.5, 1586, 1411 and 1023 (cm^{-1}). The findings revealed that the biocomposite are highly efficient adsorbent for insecticide and these might have potential applications for the adsorption of insecticide from effluents. Also, previous findings revealed similar observations, i.e., CS, PAN, starch and PPY composite with bagasse, which promising efficiency for the elimination of dye (Noreen et al., 2020). On similarly, composite of PAN

and Na-Alg with *Oscillatoria* biomass was fabricated and used for the adsorptive removal of basic blue 41, which furnished excellent efficient as an adsorbent (Maqbool et al., 2020). Also, PPY, PAN and Na-Alg composites furnished excellent adsorptive elimination of insecticide (Ishtiaq et al., 2020). The enhanced adsorptive capacity of the biocomposite is due to the changes in physicochemical properties, i.e., mechanical properties may enhance due to chemical interaction in the polymer chains and resultantly, the adsorbent became rigid and unable to move freely, which revealed the compatibility of the composite matrix. Also, the tensile strength may enhance of the composite material. The surface area of the composite material became more effective in matrix and enhance the tensile strength of biocomposite, which resulted in better mechanical interlocking and efficient stress transfer between individual components of the matrix and resultantly, composite may offer better adsorption capacity versus individual components (Mukaffa et al., 2021).

4. Conclusions

Biocomposites of pH with PAN, PPY and Na-Alg were successfully fabricated and utilized for the adsorptive removal of NP insecticide. The optimal conditions for NP effective removal of were 30 °C, contact time 60 min, adsorbent doses 0.05 g/50 mL in the acidic pH range. Pseudo second order kinetic model and Freundlich isotherm models explained the NP adsorption biocomposites. All biocomposites presented recyclable ability with NaOH eluting agent and found to be promising adsorbents for the elimination of NP from aqueous medium. Prepared biocomposites displayed high affinity for the biosorption of insecticide and this class of adsorbents could can be utilized for the remediation of insecticide in effluents.

Declaration of Competing Interest

The authors declare that they have no known competing financial interests or personal relationships that could have appeared to influence the work reported in this paper.

Acknowledgements

This research was funded by the Deanship of Scientific Research at Princess Nourah bint Abdulrahman University through the Fast-track Research Funding Program.

References

Abbas, N., Butt, M.T., Ahmad, M.M., Deeba, F., Hussain, N., 2021. Phytoremediation potential of Typha latifolia and water hyacinth for removal of heavy metals from industrial wastewater. Chem. Int. 7, 103–111.

Adetutu, I.A., Iwuoha, G.N., Michael Jnr, H., 2020. Carcinogenicity of dioxin-like polychlorinated biphenyls in transformer soil in vicinity of University of Port Harcourt, Choba, Nigeria. Chem. Int. 6, 144–150.

Amer, M.W., Awwad, A.M., 2021. Green synthesis of copper nanoparticles by *Citrus limon* fruits extract, characterization and antibacterial activity. Chem. Int. 7, 1–8.

Awwad, A.M., Amer, M.W., Salem, N.M., Abdeen, A.O., 2020a. Green synthesis of zinc oxide nanoparticles (ZnO-NPs) using *Ailanthus altissima* fruit extracts and antibacterial activity. Chem. Int. 6, 151–159.

Awwad, A.M., Maisa'a, W., Amer, M.W., 2021a. $Fe(OH)_3$/kaolinite nanoplatelets: Equilibrium and thermodynamic studies for the adsorption of Pb(II) ions from aqueous solution. Chem. Int. 7, 90–102.

Awwad, A.M., Salem, N.M., Amer, M.W., Shammout, M.a.W., 2021. Adsorptive removal of Pb(II) and Cd (II) ions from aqueous solution onto modified Hiswa iron-kaolin clay: Equilibrium and thermodynamic aspects. Chem. Int. 7, 139–144.

Awwad, A.M., Salem, N.M., Aqarbeh, M.M., Abdulaziz, F.M., 2020b. Green synthesis, characterization of silver sulfide nanoparticles and antibacterial activity evaluation. Chem. Int. 6, 42–48.

Benabdallah, N., Harrache, D., Mir, A., De La Guardia, M., Benhachem, F., 2017. Bioaccumulation of trace metals by red alga Corallina elongata in the coast of Beni Saf, west coast, Algeria. Chem. Int 3, 220–231.

Bhatti, H.N., Mahmood, Z., Kausar, A., Yakout, S.M., Shair, O.H., Iqbal, M., 2020. Biocomposites of polypyrrole, polyaniline and sodium alginate with cellulosic biomass: Adsorption-desorption, kinetics and thermodynamic studies for the removal of 2,4-dichlorophenol. Int. J. Biol. Macromol. 153, 146–157.

Bokhari, T.H., Ahmad, N., Jilani, M.I., Saeed, M., Usman, M., Haq, A.U., Rehman, R., Iqbal, M., Nazir, A., Javed, T., 2020. UV/H_2O_2, UV/H_2O_2/SnO_2 and Fe/H_2O_2 based advanced oxidation processes for the degradation of disperse violet 63 in aqueous medium. Mater. Res. Exp. 7, 015531.

Dai, Z.-L., Yang, W.-L., Fan, Z.-X., Guo, L., Liu, Z.-H., Dai, Y.-J., 2021. Actinomycetes Rhodococcus ruber CGMCC 17550 degrades neonicotinoid insecticide nitenpyram via a novel hydroxylation pathway and remediates nitenpyram in surface water. Chemosphere 270, 128670.

Daij, K.B., Bellebia, S., Bengharez, Z., 2017. Comparative experimental study on the COD removal in aqueous solution of pesticides by the electrocoagulation process using monopolar iron electrodes. Chem. Int. 3, 420–427.

Demarchi, C.A., Debrassi, A., de Campos Buzzi, F., Nedelko, N., Ślawska-Waniewska, A., Dłużewski, P., Dal Magro, J., Scapinello, J., Rodrigues, C.A., 2019. Adsorption of the dye Remazol Red 198 (RR198) by O-carboxymethylchitosan-N-lauryl/γ-Fe_2O_3 magnetic nanoparticles. Arab. J. Chem. 12, 3444–3453.

Djehaf, K., Bouyakoub, A.Z., Ouhib, R., Benmansour, H., Bentouaf, A., Mahdad, A., Moulay, N., Bensaid, D., Ameri, M., 2017. Textile wastewater in Tlemcen (Western Algeria): Impact, treatment by combined process. Chem. Int. 3, 414–419.

Dubinin, M., Raduskhevich, L., 1947. Proceedings of the academy of sciences of the USSR. Phys. Chem. 55, 327–329.

Elsherif, K.M., El-Dali, A., Alkarewi, A.A., Mabrok, A., 2021. Adsorption of crystal violet dye onto olive leaves powder: Equilibrium and kinetic studies. Chem. Int. 7, 79–89.

Freundlich, H., 1906. Over the adsorption in solution. J. Phys. Chem. 57, 1100–1107.

Gupta, R., Singh, R., Dubey, S., 2004. Removal of mercury ions from aqueous solutions by composite of polyaniline with polystyrene. Sep. Purif. Technol. 38, 225–232.

Harkins, W.D., Jura, G., 1944. Surfaces of solids. XIII. A vapor adsorption method for the determination of the area of a solid without the assumption of a molecular area, and the areas occupied by nitrogen and other molecules on the surface of a solid. J. Am. Chem. Soc. 66, 1366–1373.

Ho, Y.-S., McKay, G., 1999. Pseudo-second order model for sorption processes. Proces. Biochem. 34, 451–465.

Igbanoi, F.J., Ihunda, I.E., Iwuoha, G.N., 2019. Leachates and physicochemical characteristics of Rumuodumaya dumpsites, Niger-Delta, Nigeria. Chem. Int. 5, 126–131.

Iqbal, M., Abbas, M., Nazir, A., Qamar, A.Z., 2019. Bioassays based on higher plants as excellent dosimeters for ecotoxicity monitoring: A review. Chem. Int. 5, 1–80.

Iqbal, M., Khera, R.A., 2015. Adsorption of copper and lead in single and binary metal system onto Fumaria indica biomass. Chem. Int. 1, 157b–163b.

Ishtiaq, F., Bhatti, H.N., Khan, A., Iqbal, M., Kausar, A., 2020. Polypyrole, polyaniline and sodium alginate biocomposites and adsorption-desorption efficiency for imidacloprid insecticide. Int. J. Biol. Macromol. 147, 217–232.

Ismail, R.M., Almaqtri, W.Q., Hassan, M., 2021. Kaolin and bentonite catalysts efficiencies for the debutylation of 2-tert-butylphenol. Chem. Int. 7, 21–29.

Jamal, M.A., Muneer, M., Iqbal, M., 2015. Photo-degradation of monoazo dye blue 13 using advanced oxidation process. Chem. Int. 1, 12–16.

Jamil, A., Bokhari, T.H., Iqbal, M., Bhatti, I.A., Zuber, M., Nisar, J., Masood, N., 2020a. Gamma radiation and hydrogen peroxide based advanced oxidation process for the degradation of disperse dye in aqueous medium. Z. Phys. Chem. 234, 279–294.

Jamil, A., Bokhari, T.H., Iqbal, M., Zuber, M., Bukhari, I.H., 2020b. $ZnO/UV/H_2O_2$ based advanced oxidation of disperse red dye. Z. Phys. Chem. 234, 129–143.

Jamil, A., Bokhari, T.H., Javed, T., Mustafa, R., Sajid, M., Noreen, S., Zuber, M., Nazir, A., Iqbal, M., Jilani, M.I., 2020c. Photocatalytic degradation of disperse dye Violet-26 using TiO2 and ZnO nanomaterials and process variable optimization. J. Mater. Res. Technol. 9, 1119–1128.

Kovačević, Z., Bischof, S., Vujasinović, E., Fan, M., 2019. The influence of pre-treatment of Spartium junceum L. fibres on the structure and mechanical properties of PLA biocomposites. Arab. J. Chem. 12, 449–463.

Lagergren, S., 1898. Zur theorie der sogenannten adsorption gel Zur theorie der sogenannten adsorption gelster stoffe. Kungliga Svenska Vetenskapsakademiens, Handlingar 24, 1–39.

Langmuir, I., 1918. The adsorption of gases on plane surfaces of glass, mica and platinum. J. Am. Chem. Soc. 40, 1361–1403.

Lee, Y.-J., Kang, J.-K., Park, S.-J., Lee, C.-G., Moon, J.-K., Alvarez, P.J.J., 2020. Photocatalytic degradation of neonicotinoid insecticides using sulfate-doped Ag_3PO_4 with enhanced visible light activity. Chem. Eng. J. 402, 126183.

Maqbool, M., Bhatti, H.N., Sadaf, S., Al-Anazy, M.m., Iqbal, M., 2020. Biocomposite of polyaniline and sodium alginate with Oscillatoria biomass: A potential adsorbent for the removal of basic blue 41. J. Mater. Res. Technol. 9, 14729–14741.

Marinescu, C., Sofronia, A., Anghel, E.M., Baies, R., Constantin, D., Seciu, A.-M., Gingu, O., Tanasescu, S., 2019. Microstructure, stability and biocompatibility of hydroxyapatite – titania nanocomposites formed by two step sintering process. Arab. J. Chem. 12, 857–867.

Mukaffa, H., Asrofi, M., Sujito, Asnawi, Hermawan, Y., Sumarji, Qoryah, R.D.H., Sapuan, S.M., Ilyas, R.A., Atiqah, A., 2021. Effect of alkali treatment of piper betle fiber on tensile properties as biocomposite based polylactic acid: Solvent cast-film method. Mater. Today: Proc., https://doi.org/10.1016/j.matpr.2021.1002.1218.

Noreen, S., Bhatti, H.N., Iqbal, M., Hussain, F., Sarim, F.M., 2020. Chitosan, starch, polyaniline and polypyrrole biocomposite with sugarcane bagasse for the efficient removal of Acid Black dye. Int. J. Biol. Macromol. 147, 439–452.

Palanisamy, P., Agalya, A., Sivakumar, P., 2012. Polymer composite—a potential biomaterial for the removal of reactive dye. J. Chem. 9, 1823–1834.

Qureshi, K., Ahmad, M., Bhatti, I., Iqbal, M., Khan, A., 2015. Cytotoxicity reduction of wastewater treated by advanced oxidation process. Chem. Int. 1, 59.

Ramli, N.H., Yusup, S., Quitain, A.T., Johari, K., Kueh, B.W.B., 2019. Optimization of saponin extracts using microwave-assisted extraction as a sustainable biopesticide to reduce Pomacea canaliculata population in paddy cultivation. Sustain. Chem. Pharm. 11, 23–35.

Sasmaz, M., Obek, E., Sasmaz, A., 2018. The accumulation of La, Ce and Y by Lemna minor and Lemna gibba in the Keban gallery water, Elazig Turkey. Water Environ. J. 32, 75–83.

Sasmaz, M., Öbek, E., Sasmaz, A., 2019. Bioaccumulation of cadmium and thallium in Pb-Zn tailing waste water by Lemna minor and Lemna gibba. Appl. Geochem. 100, 287–292.

Sayed, M., 2015. Removal of ciprofloxacin by gamma irradiation: Degradation mechanism and pathways of products studies. Chem. Int. 1, 81–86.

Shoukat, S., Bhatti, H.N., Iqbal, M., Noreen, S., 2017. Mango stone biocomposite preparation and application for crystal violet adsorption: A mechanistic study. Micropor. Mesopor. Mater. 239, 180–189.

Sinanoglu, D., Sasmaz, A., 2019. Geochemical evidence on the depositional environment of Nummulites accumulations around Elazig, Sivas, and Eskişehir (Turkey) in the middle Eocene subepoch. Arab. J. Geosci. 12, 759.

Sohail, I., Bhatti, I.A., Ashar, A., Sarim, F.M., Mohsin, M., Naveed, R., Yasir, M., Iqbal, M., Nazir, A., 2020. Polyamidoamine (PAMAM) dendrimers synthesis, characterization and adsorptive removal of nickel ions from aqueous solution. J. Mater. Res. Technol. 9, 498–506.

Tahir, N., Bhatti, H.N., Iqbal, M., Noreen, S., 2017. Biopolymers composites with peanut hull waste biomass and application for Crystal Violet adsorption. Int. J. Biol. Macromol. 94, 210–220.

Tang, M., Ao, Y., Wang, C., Wang, P., 2020. Rationally constructing of a novel dual Z-scheme composite photocatalyst with significantly enhanced performance for neonicotinoid degradation under visible light irradiation. Appl. Catal. B 270, 118918.

Temkin, M., 1940. Kinetics of ammonia synthesis on promoted iron catalysts. Acta Phys. URSS 12, 327–356.

Ukpaka, C.P., Eno, O.N., 2020. Modeling of Azadirachta indica leaves powder efficiency for the remediation of soil contaminated with crude oil. Chem. Int. 7, 62–70.

Ukpaka, C.P., Lezorghia, S.B., Nwosu, H., 2020. Crude oil degradation in loamy soil using Neem root extracts: An experimental study. Chem. Int. 6, 160–167.

Weber, W.J., Morris, J.C., 1963. Kinetics of adsorption on carbon from solution. J. Sanit. Eng. div. 89, 31–60.

Wu, X., Zhang, X., Zhang, H., Zhang, G., Fei, Z., 2014. Adsorption of Nitenpyram and Acetamiprid on Modified Resin with Proline. Asian J. Chem. 26, 303.

Yuan, M., Liu, X., Li, C., Yu, J., Zhang, B., Ma, Y., 2019. A higher efficiency removal of neonicotinoid insecticides by modified cellulose-based complex particle. Int. J. Biol. Macromol. 126, 857–866.